LANGMUIR

Article

pubs.acs.org/Langmuir

Adsorption of Butanol and Water Vapors in Silicalite-1 Films with a Low Defect Density

Amirfarrokh Farzaneh,[†] Ming Zhou,[†] Oleg N. Antzutkin,[‡,§] Zoltán Bacsik,[∥] Jonas Hedlund,[†] Allan Holmgren,[†] and Mattias Grahn*[,†]

[†]Chemical Technology and [‡]Chemistry of Interfaces, Luleå University of Technology, SE-971 87 Luleå, Sweden

[§]Department of Physics, Warwick University, CV4 7AL Coventry, United Kingdom

[∥]Department of Materials and Environmental Chemistry, Stockholm University, SE-106 91 Stockholm, Sweden

Supporting Information

ABSTRACT: Pure silica zeolites are potentially hydrophobic and have therefore been considered to be interesting candidates for separating alcohols, e.g., 1-butanol, from water. Zeolites are traditionally synthesized at high pH, leading to the formation of intracrystalline defects in the form of silanol defects in the framework. These silanol groups introduce polar adsorption sites into the framework, potentially reducing the adsorption selectivity toward alcohols in alcohol/water mixtures. In contrast, zeolites prepared at neutral pH using the fluoride route contain significantly fewer defects. Such crystals should show a much higher butanol/water selectivity than crystals prepared in traditional hydroxide (OH^-) media. Moreover, silanol groups are present at the external surface of the zeolite crystals; therefore, minimizing the external surface of the studied adsorbent is important. In this work, we determine adsorption isotherms of 1-butanol and water in silicalite-1 films prepared in a fluoride (F^-) medium using in situ attenuated total reflectance−Fourier transform infrared (ATR−FTIR) spectroscopy. This film was composed of well intergrown, plate-shaped *b*-oriented crystals, resulting in a low external area. Single-component adsorption isotherms of 1-butanol and water were determined in the temperature range of 35−80 °C. The 1-butanol isotherms were typical for an adsorbate showing a high affinity for a microporous material and a large increase in the amount adsorbed at low partial pressures of 1-butanol. The Langmuir−Freundlich model was successfully fitted to the 1-butanol isotherms, and the heat of adsorption was determined. Water showed a very low affinity for the adsorbent, and the amounts adsorbed were very similar to previous reports for large silicalite-1 crystals prepared in a fluoride medium. The sample also adsorbed much less water than did a reference silicalite-1(OH^-) film containing a high density of internal defects.The results show that silicalite-1 films prepared in a F^- medium with a low density of defects and external area are very promising for the selective recovery of 1-butanol from aqueous solutions.

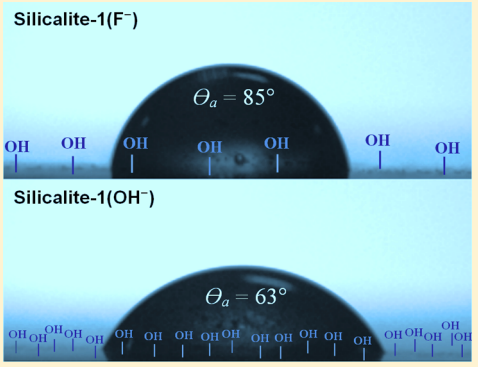

INTRODUCTION

Microporous zeolite-type materials have already been used in laboratory- to industrial-scale adsorptive separation processes.[1] One of the key properties of zeolites that controls the selectivity in adsorptive separation is the silicon to aluminum (Si/Al) ratio of the framework, which can be adjusted during the hydrothermal synthesis.[2] The property of zeolites to selectively adsorb nonpolar and low-polarity molecules in the presence of water increases with increasing Si/Al ratio. Consequently, zeolites with low aluminum content and their aluminum-free analogs are known as potential adsorbents in applications concerning the recovery of organic chemicals from water.[3] The separation of alcohols (including 1-butanol) from low-concentration aqueous solutions is an important challenge for bioalcohol production via fermentative processes, and over the last few decades, the application of high-silica zeolites for alcohol/water separation has made great progress, with membrane-based separations gaining in interest lately.[4−8] In particular, high silica MFI-type zeolites and their pure silica analog, silicalite-1, can selectively adsorb alcohols from dilute aqueous solutions.[9−13] Other promising materials for this separation of recent interest include metal−organic frameworks, e.g., ZIF-8, and activated carbons.[14−16] These materials all have their pros and cons regarding their properties (saturation capacities, diffusivities of adsorbates, regeneration temperature, long-term stability, etc.) for applications in separating butanol from dilute aqueous mixtures, and the findings reported in the literature are often conflicting.[14−21]

Several research groups have studied the recovery of 1-butanol (hereinafter referred to as butanol) from dilute aqueous solutions or real fermentation broths by high-silica MFI membranes or adsorbents.[6,9−11,17,21−24] An efficient mem-

Received: September 9, 2016
Revised: October 18, 2016
Published: October 24, 2016

DOI: 10.1021/acs.langmuir.6b03326
Langmuir 2016, 32, 11789−11798

brane-separation process should demonstrate high flux as well as sufficient selectivity. However, many papers have reported high separation factors but a low flux for alcohol/water separation.[25,26] Ultrathin MFI membranes have been used in our group for alcohol/water separation with very high fluxes and reasonably high separation factors.[27,28] For example, Yu et al.[6] studied the recovery of butanol from aqueous mixtures using ultrathin MFI membranes and reported fluxes significantly higher than previously reported, up to 40 kg m^{-2} h^{-1} and with a separation factor of 16.

Recently, DeJaco et al.[29] used Monte Carlo simulation to investigate the adsorption properties of all-silica MFI zeolites for the separation of butanol from an acetone−butanol−ethanol (ABE) fermentation broth and estimated adsorption selectivities of more than 30 000 for butanol over water. Faisal et al.[17] investigated the recovery of butanol from model fermentation broth using high-silica MFI-type zeolites and showed that the adsorbent was selective toward butanol and that the other components present in the fermentation broth had a very small effect on the amount of butanol adsorbed. In our recent work,[30] we investigated the adsorption of butanol and water from the vapor phase in a silicalite-1 film synthesized at high pH in a hydroxide medium (OH^-) using in situ attenuated total reflectance−Fourier transform infrared (ATR−FTIR) spectroscopy. We successfully measured single-component adsorption isotherms for butanol and water at different temperatures. Moreover, a binary adsorption experiment showed that the silicalite-1 film was highly butanol-selective.

Traditionally, high-silica MFI zeolites are synthesized at high pH, implying the formation of intracrystalline defects in the form of silanol groups,[31] and several studies[31−34] demonstrated a direct relationship between the number of silanol groups and the hydrophilic property of zeolites. As early as 1978, Flanigen and Patton[35] suggested a new synthesis method at nearly neutral pH using fluoride ions as mineralizing agent to prepare crystals with a low density of structural defects in the form of internal silanol groups and consequently a higher degree of hydrophobicity. More recently, several reports have emerged on the preparation of zeolites using fluoride as a mineralizing agent with a nearly defect-free structure.[34,36−38] For example, Qin et al.[39] reported the seeded synthesis of nano-ZSM-5-type zeolites in both OH^- and F^- media. Their IR and NMR characterization of these zeolites proved that the fraction of framework defects in the ZSM-5(F^-) samples was significantly smaller than the corresponding fraction in the reference ZSM-5(OH^-) samples. Recently, our group reported the preparation of colloidal silicalite-1 single crystals[34] prepared in a F^- medium at nearly neutral pH with an almost defect-free lattice structure. These small crystals showed a much higher alcohol/water adsorption selectivity than did silicalite-1 crystals prepared in an OH^- medium.

Therefore, aluminum-free MFI zeolites prepared with F^- as a mineralizing agent seem to be excellent candidates for the separation of alcohols from aqueous mixtures. However, literature data on the adsorption properties of silicalite-1(F^-) for alcohol/water separation is still scarce, but Zhang et al.[33] published a comprehensive study of the adsorption of water and ethanol in high-silica and pure-silica MFI-type zeolites and showed that silicalite-1 synthesized via the fluoride medium was the most promising candidate for the recovery of ethanol from dilute aqueous solutions. They reported a maximum water adsorption of 0.175 mmol/g for silicalite-1(F^-), which was a factor of 8 lower than the amount of water adsorbed in the traditional silicalite-1(OH^-). Zhou et al.[40] investigated the butanol/water separation performance of a thin MFI membrane grown on an α-alumina support in the fluoride medium and reported a high separation factor of 19. However, they used OH^--synthesized crystals for the seeding of the membrane, so the membrane could potentially contain some defects that reduced the separation performance.

Albeit synthesis at neutral pH results in an almost defect-free structure for silicalite-1, silanol groups will be present on the external surface of the crystals.[41] To reduce this influence on the adsorption properties of a zeolite film, the external surface of the film should be minimized by arranging crystals in a uniformly oriented monolayer of large crystals to minimize capillary condensation between crystals in grain boundaries.

The aim of the current work was to study the adsorption of butanol and water from the vapor phase in a silicalite-1 film synthesized solely, i.e., including crystals for the seeding of membranes, in the fluoride medium, thus showing a low density of structural defects.

This work is complementary to our previous work on the adsorption of the same adsorbates in a silicalite-1(OH^-) film containing a higher density of defects. The present report is, to the best of our knowledge, the first detailed report of the adsorption of butanol and water vapor silicalite-1 prepared using solely the fluoride route, and the results reported in this work may be a valuable reference on alcohol/water separation using highly hydrophobic zeolite membranes or adsorbents.

EXPERIMENTAL SECTION

Synthesis and Characterization. The synthesis mixtures for the growth of silicalite-1(F^-) seed crystals were prepared by first mixing appropriate amounts of tetraethoxysilane (TEOS, >98%, Merck) and tetrapropylammonium hydroxide (TPAOH, 40 wt %, Sigma). After shaking the mixture at room temperature for 24 h, a fully hydrolyzed clear synthesis solution was obtained. Subsequently, some of the water and most of the ethanol were removed from the solution using a rotary evaporator operated at 50 °C for about 1 h, and a thick, clear gel was obtained. After that, distilled water was added to the gel, and the gel was shaken for 24 h until a clear solution was obtained again. Thereafter, hydrofluoric acid (38−40 wt %, Merck) in an equimolar amount to TPAOH was quickly added to the synthesis mixtures at 4 °C under stirring, and after about 10 s, a very viscous, clear gel was formed with a pH value of 6.3. Under the assumption that all ethanol was removed from the mixture during evaporation, the resulting molar ratio of the very viscous, clear gel was 1 SiO_2:0.36 TPAOH:0.36 HF:11.64 H_2O. Finally, the obtained gel was transferred to a polypropylene bottle and kept at 60 °C for 2 months for the growth of the seed crystals. The silicalite-1(F^-) seed was washed four times by centrifugation and redispersion in distilled water four times and then freeze-dried before seeding.

Thin and *b*-oriented silicalite-1 films were grown on both sides of a ZnS ATR crystal (with dimensions of 50 × 20 × 2 mm and 45° cut edges, Crystran, Ltd.) by the following method. To facilitate the attachment of the seeds to the ATR crystal, both sides of the ATR crystal were coated with a thin layer of cellulosic polymer [hydroxypropylcellulose (HPC), Sigma-Aldrich, 99%] using a spin coater (2 wt % HPC dissolved in ethanol solution, and spin coating was conducted at 3000 rpm for 15 s). After drying at 105 °C for 1 h, a monolayer of silicalite-1(F^-) seed crystals was assembled on the ATR crystal by rubbing the powder of seeds onto both surfaces. The seeded ATR crystal was calcined at 500 °C for 2 h with a heating and cooling rate of 0.8 °C/min to remove the polymer layer between the silicalite-1 seeds and the ATR crystal. Thereafter, the seeded ATR crystal was kept for 6 h in a synthesis gel in an autoclave at 150 °C to grow the seed crystals into a continuous silicalite-1(F^-) film. The gel was produced in two steps: first, the precursor solution, containing TEOS

DOI: 10.1021/acs.langmuir.6b03326
Langmuir 2016, 32, 11789−11798

and TPAOH, was hydrolyzed for 12 h on a shaker, and then hydrofluoric acid, in an equimolar amount to TPAOH, was quickly added to the clear solution at 4 °C under stirring; after about 10 s, a very viscous, clear gel formed. The resulting molar ratio of the very viscous, clear gel was 1 TEOS:0.2 TPAF:20 H_2O. After synthesis, the film was thoroughly rinsed with a 0.1 M ammonia solution and dried at 50 °C overnight. Subsequently, the film was calcined at 500 °C for 2 h with a heating and cooling rate of 0.8 °C/min in order to remove the template molecules from the pores of the zeolite.

For the characterization of the film, X-ray diffraction (XRD) data were recorded using a PANalytical Empyrean instrument equipped with a PIXcel3D detector, and scanning electron microscopy (SEM) images were recorded with a FEI Magellan 400 field emission instrument.

In Situ ATR–FTIR Experiments. The ATR–FTIR quantitative technique used in this work was developed in our group and has previously been used for the adsorption of light gases and hydrocarbons in MFI films.[42−44] Spectral data were acquired with a Bruker IFS 66v/S FTIR spectrometer equipped with a deuterated triglycine sulfate (DTGS) detector and a vertical ATR accessory. The spectra were recorded by averaging 256 scans at a resolution of 4 cm^{-1}. The silicalite-1-coated ATR crystal was mounted in a heatable flow cell connected to a gas delivery system to perform the adsorption experiments. Prior to the measurements, the zeolite-coated ATR crystal was dried by heating the cell to 300 °C for 4 h with a heating and cooling rate of 0.9 °C/min under a constant flow of helium (AGA, 99.999%). After the cell was dried, a background spectrum of the film was recorded under a flow of helium. The adsorption measurements of water (distilled water) and butanol (Sigma-Aldrich 99.9%) were performed by the stepwise increase of the partial pressure of the adsorbate in the helium flow with a total pressure of 1 atm. The experimental setup and methodology used for the adsorption measurements were described in detail previously.[30,45] (For the methods, see the Supporting Information (SI).)

^{29}Si Solid-State NMR. Single-pulse ^{29}Si magic-angle-spinning (MAS) and cross-polarization (CP) MAS NMR (^{29}Si CP/MAS NMR) spectra were recorded with proton decoupling (with a nutation frequency of protons of 58 kHz) on a Varian/Chemagnetics InfinityPlus CMX-300 NMR spectrometer using a double-resonance 7.5 mm MAS probe. ^{1}H and ^{29}Si resonance frequencies were 300.103 and 59.616 MHz, respectively. The samples (63.9 mg of silicalite-1(F^-) and 53.6 mg of silicalite-1(OH^-)) were spun at 5 kHz in zirconia rotors of 7.5 mm outer diameter. 1732 (for silicalite-1(F^-)) and 816 (for silicalite-1(OH^-)) signal transients with a relaxation delay of 5 s were accumulated for single-pulse ^{29}Si MAS NMR experiments with a 90°(^{29}Si) excitation pulse length of 6.5 μs. Also, a control single-pulse ^{29}Si MAS NMR experiment with a short 30° excitation pulse of 2.2 μs, a relaxation delay of 60 s, and 784 accumulated signal transients was performed for the sample of silicalite-1(F^-) that revealed an almost identical line shape (spectrum not shown) to that in the 90°-single-pulse ^{29}Si MAS NMR spectrum of the same sample. 4036 (for silicalite-1(F^-)) and 1272 (for silicalite-1(OH^-)) signal transients with a relaxation delay of 2 s were collected for ^{29}Si CP/MAS NMR spectra. Cross-polarization (cp) from protons to ^{29}Si nuclei was performed using a ramp-cp pulse sequence with a cp-pulse length of 2.5 ms and the cp-amplitude in the X-channel (^{29}Si) ramped by 20% in 10 steps. The nutation frequency of protons during cross-polarization was 48 kHz. All parameters for the NMR experiments on silicalite-1 samples (pulse lengths, cross-polarization conditions, etc.) and external referencing of all ^{29}Si NMR spectra were obtained using a sample of a high-purity-grade kaolinite, in which ^{29}Si MAS NMR spectra clearly revealed two narrow (with line widths of ca. 35 Hz each) resonance lines at −92.3 and −91.7 ppm with respect to TMS (0 ppm). Therefore, the external reference was set at −92.0 ppm right at the saddle point between these two lines.

Contact Angle Measurement. The contact angle measurements were performed at 25 °C by using a FIBRO 1121/1122 DAT dynamic absorption and contact angle tester. During the measurements, the silicalite-1-coated ATR elements were placed horizontally in the measuring compartment and monitored by a video system. For each sample, a small volume of DI water (4 μdm^3) was placed at least four times at different locations on the surface of the silicalite-1 films. The method and data evaluation are explained in detail elsewhere.[46]

Adsorption in Silicalite-1 Powders. Water and butanol uptake in the silicalite-1(F^-) crystals used as seeds for film growth were determined for comparison to the adsorption behavior of the synthesized film as determined with ATR–FTIR spectroscopy. The adsorption experiments were conducted at 35 °C on an ASAP 2020 gas adsorption instrument (Micromeritics, Norcross, GA). Prior to the adsorption measurements, the sample was dried at 300 °C for 4 h with heating rate of 1 °C/min under dynamic vacuum conditions. The temperature was controlled using a Dewar flask together with a heating and cooling circulator.

RESULTS AND DISCUSSION

Characterization. Figure 1 shows XRD patterns for the uncoated ZnS ATR crystal as well as for the ATR crystal after

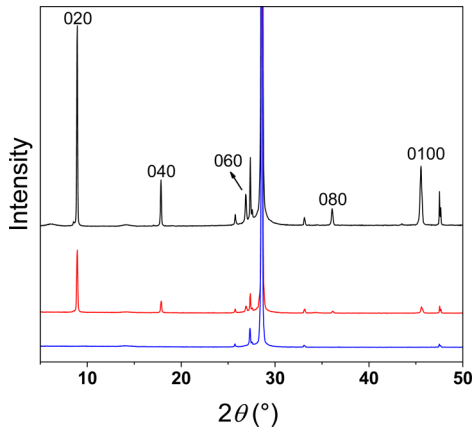

Figure 1. XRD patterns of an uncoated ZnS crystal (blue) together with the patterns for a ZnS crystal coated with a monolayer of silicalite-1(F^-) crystals (red) and a synthesized silicalite-1(F^-) film (black) in the 2θ range of 5–50°. The indexed reflections emanate from the film composed of *b*-oriented crystals.

being coated with silicalite-1(F^-) seed crystals and after film growth. For the uncoated ATR crystal, only a few reflections originating from ZnS crystals are observed. For the ATR crystal coated with a seed layer, additional reflections originating from the MFI phase are observed. Actually, only (0 *k* 0) reflections from the MFI phase are observed, which shows that the silicalite-1(F^-) seed crystals are *b*-oriented. For the sample with a silicalite-1(F^-) film, again only (0 *k* 0) reflections, but with higher intensity, are observed from the MFI phase, which shows that the film also is composed of *b*-oriented silicalite-1 crystals.

Observations by SEM support the observations by XRD. The scanning electron micrographs of the seeded ATR crystal after calcination (Figure 2a,b) show a relatively packed and uniform *b*-oriented monolayer of silicalite-1(F^-) crystals with widely varying size. The largest seed crystals have a size of about 1.0 × 0.5 × 0.1 μm^3, and as expected after calcination, no polymer layer is observed. The micrographs of the silicalite-1(F^-) film (Figure 2c,d) indicate that the seed crystals grew without secondary nucleation and formed a dense layer of *b*-oriented crystals with an average thickness of approximately 200 nm. Some of the crystals, which have been growing on top of other crystals embedded in the film, have developed a typical (for the MFI zeolite) coffin shape. The length of these crystals is as much as about 2 μm. However, most of the crystals are much

DOI: 10.1021/acs.langmuir.6b03326
Langmuir 2016, 32, 11789–11798

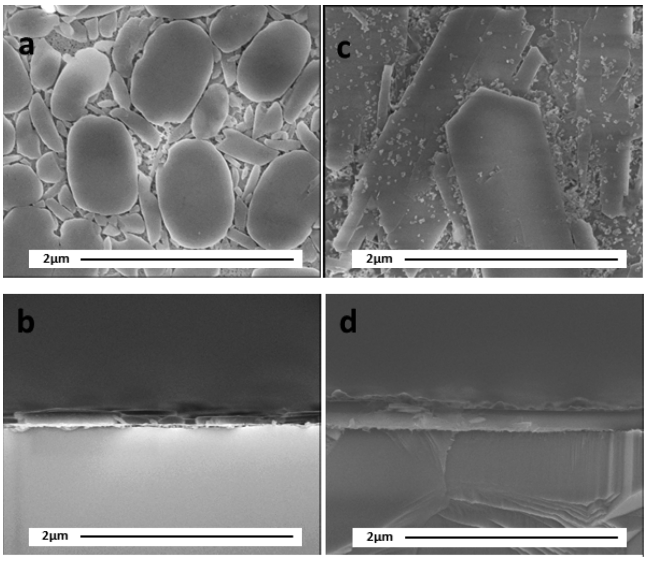

Figure 2. Top-view (a and c) and side-view (b and d) SEM images of the silicalite-1(F^-) seed layer (a and b) and synthesized film (c and d).

smaller and embedded in the film; consequently, these crystals have not developed any typical morphology.

Solid-State ^{29}Si NMR. Figure 3a,b shows single-pulse ^{29}Si MAS NMR spectra of silicalite-1(F^-), processed without

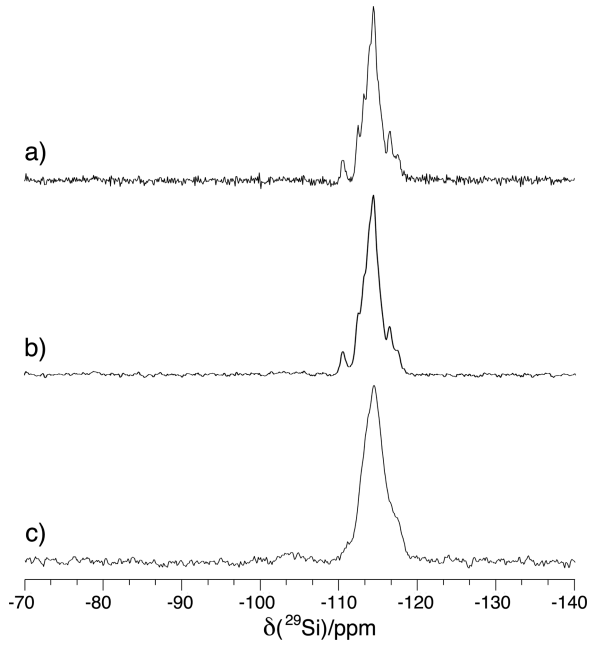

Figure 3. Single-pulse ^{29}Si MAS NMR spectra of silicalite-1(F^-) (a and b) and silicalite-1(OH^-) (c). The MAS frequency was 5 kHz. Spectrum a was processed without line broadening, whereas spectra b and c, with 10 Hz line broadening. There are 1732 signal transients in spectra a and b and 816 in spectrum c.

(Figure 3a) and with exponential line-broadening (lb = 10 Hz, see Figure 3b). Both of these differently processed spectra clearly reveal at least 9 relatively sharp (with line widths of ~0.5−1.0 ppm) overlapping resonance lines, which could be assigned to most of the 12 crystallographically distinct $Q^{(4)}$ silicon sites in the orthorhombic structure of silicalite-1.[47] A single-pulse ^{29}Si MAS NMR spectrum of the silicalite-1(OH^-) sample (Figure 3c) shows the same but considerably broader and almost featureless resonance line shape centered at ca. −114 ppm also corresponding to the same $Si(OSi)_4$ type of silicon sites in the structure of silicalite-1. In addition, a weak, broad line at ca. −103 ppm assigned to $Q^{(3)}$ Si sites in defects of the zeolite structure is also visible just above the noise level (Figure 3c). Because the ^{29}Si chemical shift is directly related to the type of Si−O−Si bonding ($Q^{(n)}$ site notation, ca. 10 ppm shift between $Q^{(n)}$ and $Q^{(n-1)}$ sites, where n = 0, 1, 2, 3 and 4) and to a lesser extent to the Si−O−Si bond angle ($\Delta\delta \approx 5$ ppm), it can be concluded that relatively well resolved ^{29}Si MAS NMR signals of silicalite-1(F^-) represent a rather well-ordered crystalline structure, which is almost free from defects (no measurable single-pulse ^{29}Si MAS NMR signals from $Q^{(3)}$ Si sites, between −100 and −105 ppm, are detected above the noise level for this sample; see Figure 3a,b). However, a poorly resolved ^{29}Si MAS NMR spectrum of silicalite-1(OH^-) is an indication of a less-crystalline structure for this sample, with local distortions in the immediate vicinity of the silicon $Q^{(4)}$ sites.[48] Such distortions may be caused by the presence of a certain number (a few % of all Si sites, estimated from the relative integral intensities of resonance lines at −114 and −103 ppm) of Si−O^- defects ($Q^{(3)}$ Si sites) detected in this sample (Figure 3c) throughout the entire structure of silicalite-1(OH^-).[49] Figure 4 represents the ^{29}Si CP/MAS NMR spectra

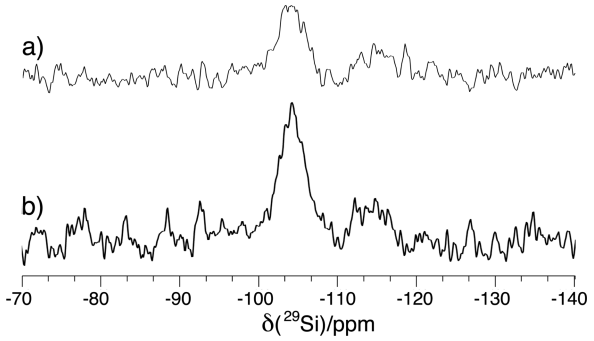

Figure 4. ^{29}Si CP/MAS NMR spectra of silicalite-1(F^-) (a) and silicalite-1(OH^-) (b). The MAS frequency was 5 kHz. Spectra were processed with 20 Hz line broadening. There are 4036 signal transients in spectrum a and 1272 in spectrum b. Spectra are mutually normalized to the weights of samples and the number of signal transients.

of the same samples of silicalite-1(F^-) (Figure 4a) and silicalite-1(OH^-) (Figure 4b), which additionally confirm the aforementioned observation of excess $Q^{(3)}$ Si defects in silicalite-1(OH^-). These two ^{29}Si CP/MAS NMR spectra are scaled so that their intensities are mutually normalized to the weights of samples and the number of signal transients (which were different for the two samples). In the ^{29}Si CP/MAS NMR experiments, magnetization is first excited at protons and then transferred to nearby ^{29}Si sites. Therefore, ^{29}Si CP/MAS NMR signals from Si−OH or/and $Si(OH)_2$ groups, in which OH protons are only two bonds distant from silicon sites, will gain the largest integral intensity, even though there are only a few % of these silicon sites in the whole sample. Obviously, the dominating signal in the ^{29}Si CP/MAS NMR spectra of silicalite-1 samples under study is at ca. −104 ppm, which was previously assigned to Si−OH ($Q^{(3)}$) groups in defects. Even a weak NMR signal (just above noise level) at ca. −115 ppm corresponding to ($Q^{(4)}$) silicon sites, which are close to Si−OH

DOI: 10.1021/acs.langmuir.6b03326
Langmuir 2016, 32, 11789−11798

groups in the silicalite-1 structure, are also detectable. A simple qualitative comparison of ^{29}Si CP/MAS NMR spectra shown in Figure 4a,b suggests that the intensity of the resonance line at ca. −104 ppm was significantly larger for the silicalite-1(OH$^-$) sample than for the silicalite-1(F$^-$) sample. Therefore, it can be concluded that the latter sample has a significantly smaller number of defects in total. For a quantitative analysis of the defects in these samples, the resonance lines at ca. −104 ppm in the direct excitation single-pulse ^{29}Si MAS NMR spectra should be integrated, which was difficult because these signals are close to the noise level (Figure 3b,c). However, even defect-free samples have hydroxyl groups on the external surface of the crystals, which will be discussed further below. Consequently, it is possible that the −104 ppm signal mostly or entirely emanates from Si−OH (Q$^{(3)}$) sites at the surface of the silicalite-1(F$^-$) crystals.

Contact Angle Measurement. The hydrophobicity of the surface of the silicalite-1 films was investigated by measuring the contact angle of water (Figure 5). Hydrophilic surfaces are

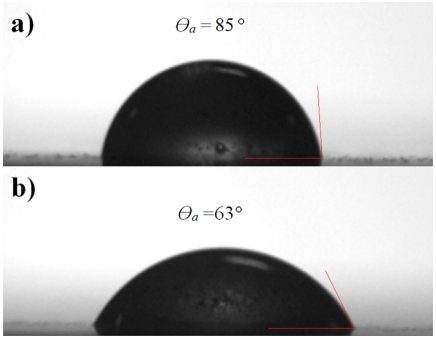

Figure 5. Illustration of the measured contact angle on the external surface of silicalite-1(F$^-$) (a) and silicalite-1(OH$^-$) (b) films.

usually defined as having a contact angle with water of less than 90°.[50] The measured contact angle is less than 90° for both samples; consequently, the external surface of both samples are per definition hydrophilic. The hydrophilic nature of the external surface of the samples should be related to the external hydroxyl groups that will be present at the surface even for defect-free samples.[41] The contact angle between water and the silicalite-1(F$^-$) surface was 85 ± 2°, whereas for the silicalite-1(OH$^-$) sample, which was investigated in our previous work,[30] the contact angle was 63 ± 2°. The much lower contact angle for the silicalite-1(OH$^-$) sample indicates the presence of additional hydroxyl groups on the surface, presumably from defects in the lattice. It should be noted that the surface roughness of the sample may affect the contact angle measurements. For a hydrophilic material (defined as a material where the contact angle with water is <90°), the surface roughness decreases the measured contact angle.[51] From the SEM images of our samples, the silicalite-1(F$^-$) sample seems to have a rougher surface than the silicalite-1(OH$^-$) sample; however, the contact angle is still higher for the silicalite-1(F$^-$) sample. We therefore conclude that the surface roughness is not responsible for the observed difference in contact angle between the two samples.

ATR-FTIR Experiments. Figure 6 shows IR spectra of butanol adsorbed in the silicalite-1(F$^-$) film at 35 °C at three different partial pressures. The spectra show the characteristic CH_3 and CH_2 stretching vibrational bands at 3000−2800 cm^{-1} originating from butanol adsorbed in the film.[30,52] The bands at

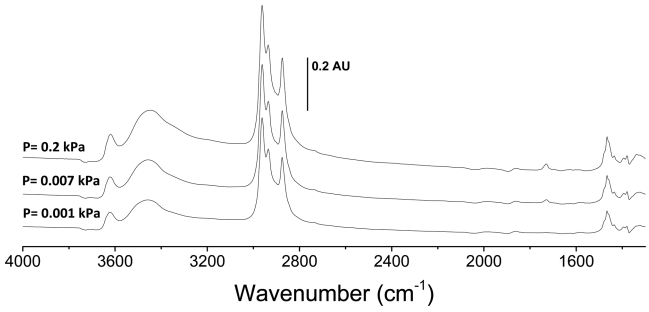

Figure 6. IR spectra of butanol adsorbed in silicalite-1(F$^-$) at 35 °C at different partial pressures as indicated.

1465 and 1380 cm^{-1} were assigned to bending vibrational modes of CH_2 and CH_3, respectively. The broad band in the range of 3700−2700 cm^{-1} originates from the O−H stretching vibration of hydrogen-bonded and non-hydrogen-bonded butanol molecules adsorbed in the film. Obviously, the intensity of the bands associated with butanol adsorbed in the silicalite-1(F$^-$) film increased with increasing partial pressure of butanol in the feed as more butanol is adsorbed at higher partial pressures. These spectra are very similar in appearance to those reported previously for butanol adsorbed in a silicalite-1(OH$^-$) film.[30]

Butanol vapor adsorption isotherms for a silicalite-1(F$^-$) film were extracted from IR spectra (by using the area under the absorption line in the range of 3000−2800 cm^{-1}) and are shown in Figure 7, with both linear (a) and logarithmic (b) pressure scales. The fitted Sips (also called the Langmuir−Freundlich) model[53] (eq 1) is also shown in the figure, as well as an adsorption isotherm determined for silicalite-1(F$^-$) crystals using the volumetric gas adsorption measurement. The Langmuir model is probably the most common model used to describe the adsorption of gases (or vapors) in microporous adsorbents such as zeolites. However, the Sips model, which is a combination of the Langmuir and Freundlich isotherms for predicting heterogeneous adsorption systems, resulted in a better fit to the experimental data than the Langmuir model. (Langmuir and Sips models fitted to experimental data for the adsorption of butanol in silicalite-1(F$^-$) as well as for adsorption in silicalite-1(OH$^-$) obtained from our previous work[30] are presented in the SI.) The Sips model is given by eq 1.

$$q = q_{sat}\frac{bp^{1/n}}{1 + bp^{1/n}} \quad (1)$$

In this equation, q_{sat} is the saturation loading (mmol/g), p is the partial pressure of the adsorbate in the gas phase (kPa), b is the Langmuir affinity parameter (kPa^n), and n is the Freundlich exponent (heterogeneity factor) that is the additional parameter in the Sips model compared to the Langmuir model and is greater than unity. If the Freundlich exponent (n) is unity, then the Langmuir equation, which is commonly applicable to ideal surfaces, will be recovered.[54] Thus, the larger the Freundlich exponent, the greater the heterogeneity of the system. The isotherm determined for the powder sample by volumetric gas adsorption measurements at 35 °C was used for calibrating the FTIR−ATR measurements. This isotherm is typical for adsorption in microporous materials, with a sharp increase in the amount adsorbed at low partial pressures. At higher partial pressures above ca. 0.1 kPa, the amount of

DOI: 10.1021/acs.langmuir.6b03326
Langmuir 2016, 32, 11789−11798

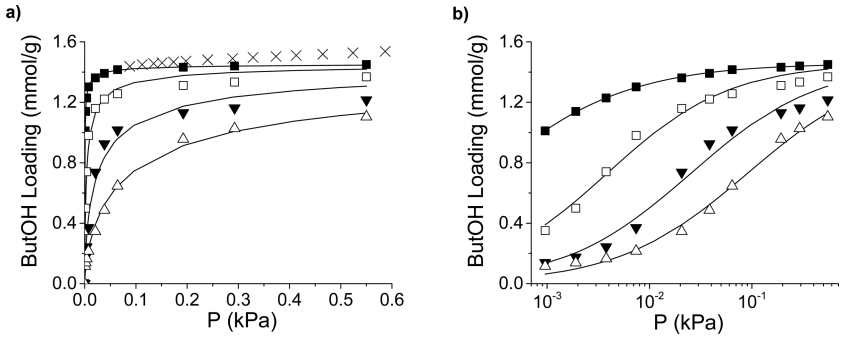

Figure 7. Adsorption isotherms on linear (a) and logarithmic (b) scales for butanol in a silicalite-1(F^-) film at (■) 35, (□) 50, (▼) 65, and (△) 80 °C, obtained from FTIR experiments and in silicalite-1(F^-) powder at 35 °C (×) obtained from volumetric measurements. Symbols and solid lines represent experimental data and the Sips model fitted to the experimental data, respectively.

butanol adsorbed leveled off and increased only slowly with increasing partial pressure of butanol, probably as a result of capillary condensation in the voids of the crystals powder.[55] On the contrary, the isotherm determined for the film at 35 °C is nearly horizontal at partial pressures above ca. 0.1 kPa, probably because of the much smaller amount of capillary condensation in the film composed of a monolayer of relatively large crystals. The saturation loading in the Sips model was therefore used as the loading before the onset of capillary condensation, i.e., at a butanol pressure of ca. 0.1 kPa. The corresponding saturation loading was consequently set to 1.46 mmol/g (Figure 7). The maximum loading of butanol measured in this work is within the same range as in previous literature reports (1.3−2 mmol/g).[17,30,56]

The adsorption isotherms determined using the film as an adsorbent are also typical for adsorption in microporous materials and are very similar to previously reported data.[21−23,30] However, an important difference is that our isotherm determined at 35 °C is nearly horizontal at partial pressures above ca. 0.1 kPa, which is not the case for isotherms of powders.[33,57] Furthermore, the Sips model fits the experimental data well. The fitted Sips parameters are presented in Table 1.

Table 1. Saturation Loadings (q_{sat}, mmol/g) and Sips Adsorption Parameters (b and n) for Butanol in Silicalite-1(F^-)

adsorbate	temp (°C)	q_{sat} (mmol/g)	b(kPa^n)	n
butanol	35	1.46	172.22	1.61
	50	1.46	57.03	1.34
	65	1.46	13.17	1.42
	80	1.46	5.17	1.46

The Langmuir affinity parameter (b) and the van't Hoff equation were used to determine the isosteric heat of adsorption at a fractional loading of 0.5[54]

$$\frac{\partial \ln b}{\partial T} = \frac{\Delta H_{ads}}{R} \quad (2)$$

where ΔH_{ads} is the isosteric heat of adsorption, R is the gas constant, and T is the absolute temperature. On the basis of the van't Hoff equation (eq 2), the isosteric heat of adsorption was determined to be −72 kJ/mol using the Langmuir affinity parameter (b) from all four isotherms, with an R^2 value of 0.995. Table 2 shows the values for the heat of adsorption of butanol determined in the present work together with the data previously reported in the literature. Literature data (such as the heat of adsorption and Langmuir and Sips parameters) on the adsorption of butanol vapor in similar adsorbents as in this work is very scarce. However, the enthalpy value obtained in this work is in concert with previous reports on similar adsorbent/adsorbate systems where the values of the heat of adsorption range from ca. −40 to −69 kJ/mol. The value obtained in this work is similar to the value in our previous report on the adsorption of butanol in silicalite-1(OH^-) (−69 kJ/mol). (See the SI for more data on the heat of adsorption of butanol in silicalite-1 films.[30])

Table 2. Heat of Adsorption of Butanol in This Work and from Literature Data

adsorbent	ΔH_{ads}(kJ/mol)	reference
silicalite-1(F^-)	−72	this work
silicalite-1(OH^-)	−69	our previous work[30]
ZIF-8	−40	Zhang et al.[33]
Na-ZSM-5 (butanol in liquid phase)	−50	Einicke et al.[58]

The IR spectra of water adsorbed in the silicalite-1(F^-) film at 35 °C and different partial pressures are shown in Figure 8.

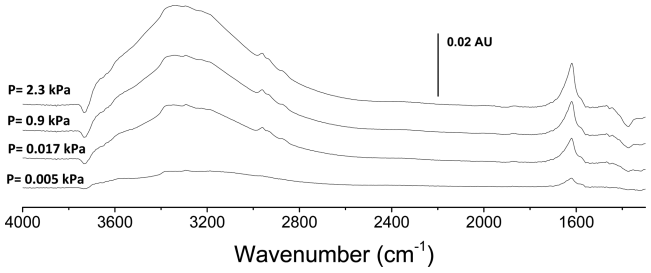

Figure 8. IR spectra of water adsorbed in silicalite-1(F^-) at 35 °C and different partial pressures.

The intensity of the bands increased with increasing partial pressure of water in the feed, showing that more water is adsorbed at higher partial pressures in the feed, as expected. The band with a peak maximum at about 1620 cm^{-1} was assigned to the bending vibration of water,[59] and the broad band in the 3700−2700 cm^{-1} range with a peak maximum at about 3370 cm^{-1} originates from O−H stretching vibrational modes (asymmetric and symmetric) of adsorbed water. The broadness of the OH stretching band indicates different strengths of hydrogen-bonding interactions experienced by water molecules in the silicalite-1 structure or at the external

DOI: 10.1021/acs.langmuir.6b03326
Langmuir 2016, 32, 11789−11798

surface. A lower wavenumber is expected for a stronger hydrogen bond, whereas the opposite is true for the bending vibration of water. Previously, we observed the peak originating from water molecules in the pore structure of the silicalite-1(OH^-) film[30] with a maximum at 1650 cm^{-1}, which indicates a stronger interaction between water molecules and the silicalite-1(OH^-) surface compared to that of silicalite-1(F^-), reflecting the strong interaction between water and the polar silanol groups in the silicalite-1(OH^-) film. The negative band at ca. 3730 cm^{-1} was assigned to the O−H stretching vibration of silanol groups at the external surface with water hydrogen bonded to these silanol groups. Free silanol groups on the external surface typically show an absorption band at ca. 3740 cm^{-1}.[60] As water adsorbs on these groups, the band is shifted to lower wavenumbers, and in this case, the band merges with the broad stretching vibrational band observed for hydrogen-bonded water.[42,59]

The quantity of water adsorbed in the silicalite-1(F^-) film was extracted from the IR spectra by integrating the area of the water deformation band at 1620 cm^{-1} using the method presented in the SI. Figure 9 shows water vapor isotherms at

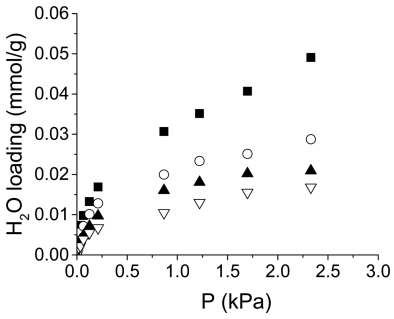

Figure 9. Adsorption isotherms for water vapor in silicalite-1(F^-) film at (■) 35 °C, (○) 50 °C, (▲) 65 °C, and (▽) 80 °C, obtained from FTIR experiments.

four different temperatures in the range 35−80 °C for adsorption in the silicalite-1(F^-) film as obtained from infrared spectra. As expected, the amount of water adsorbed in the film was much lower at higher temperatures and the adsorption increased with increasing partial pressure of water vapor in the feed.

Because of the low density of structural defects in the silicalite-1(F^-) as evidenced by ^{29}Si MAS NMR measurements, most of the silanol groups should be terminal ones on the external surface of the crystals, and the film should therefore be quite hydrophobic and certainly more so than for silicalite-1(OH^-) containing a much higher density of internal silanol groups. Indeed, the amount of water adsorbed in the silicalite-1(F^-) film was significantly lower than the amount previously reported for the silicalite-1(OH^-) film at similar conditions.[30] As an example, at 35 °C and a partial pressure of water of 0.87 kPa, the amount of water adsorbed in the silicalite-1(F^-) film was 0.03 mmol/g, whereas under the same conditions, the amount of water adsorbed in the silicalite-1(OH^-) film was 0.59 mmol/g, i.e., a 20-fold larger value (Figure 9). This clearly demonstrated the lower affinity toward water for the silicalite-1(F^-) sample than for silicalite-1(OH^-). Sorption of water in high-silica MFI has been reported to occur via a mechanism where the water molecules form clusters inside the pores.[59] Such adsorption behavior is not expected to be captured well by the Langmuir or Sips models; consequently, we did not attempt to fit these models to the experimental data for water adsorption in our silicalite-1(F^-) film.

Adsorption isotherms of water vapor at 35 °C for the two types of silicalite-1 powders (silicalite-1(F^-) and silicalite-1(OH^-)) as well as for the corresponding films were experimentally determined in our laboratory and are shown in Figure 10 together with the data reported by Zhang et al.[33]

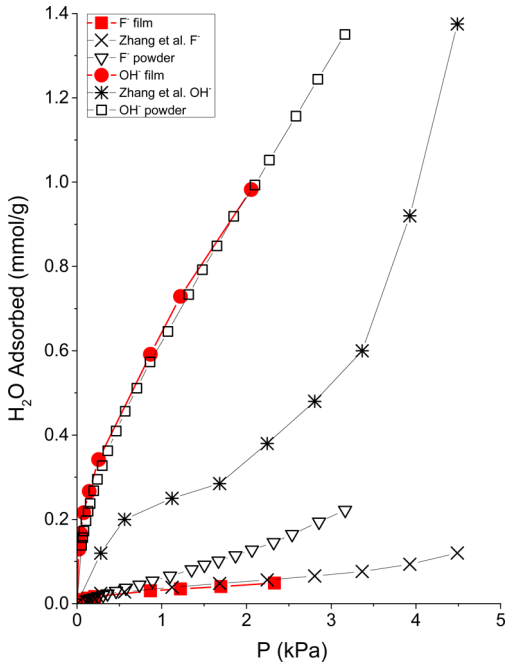

Figure 10. Experimentally determined water adsorption isotherms for silicalite-1 films and powders studied in this work together with the water isotherms in silicalite-1 powders reported by Zhang et al.[33] (All of the isotherms were measured at 35 °C.)

As expected, the amount of water adsorbed in silicalite-1(F^-) is significantly lower (~7-fold) than that for silicalite-1(OH^-), which is again in very good agreement with ^{29}Si MAS NMR results indicating a lower density of polar silanol groups in silicalite-1(F^-). Both of the silicalite-1 powder samples used in this work had slightly higher water uptake compare to those reported by Zhang et al.[33] This is probably due to the much smaller crystal size of our samples (1.0 × 0.5 × 0.1 μm^3) compared to that of Zhang et al. (70 × 30 × 15 μm^3); consequently, our samples have a larger external/internal area ratio and therefore a greater number of external silanol groups per gram of sample compared to the powder samples studied by Zhang et al. The observed difference is thus likely an effect of the larger external area available for adsorption on our powders of smaller crystals. However, the amount of water adsorbed in the film was about 3 times smaller than that for silicalite-1(F^-) powder. The reason is most likely fewer external silanol groups being exposed to water vapor for the well intergrown film compared to the crystals in the powder, which were also used as seeds for film growth. The same difference between powder and film was not observed for silicalite-1(OH^-) where the adsorption of water was very similar for both film and powder samples. In the latter samples, a majority of the silanol groups are likely internal; therefore, the contribution from adsorption on silanol groups on the external surface becomes negligible in comparison. Consequently, the adsorption behavior of water is very similar for both samples.

DOI: 10.1021/acs.langmuir.6b03326
Langmuir 2016, 32, 11789−11798

The small amount of water adsorbed in silicalite-1(F^-) film was very similar to the previous report by Zhang et al.[33] for a powder of comparatively large crystals, and these amounts are, to the best of our knowledge, the smallest amounts reported from experiments on MFI-type zeolites. The low water adsorption observed for the silicalite-1 (F^-) film together with the high affinity for butanol implies that a very high butanol/water adsorption selectivity would be expected for this type of film. Therefore, an additional experiment was carried out by exposing the silicalite-1(F^-) film to a butanol/water vapor mixture with a molar composition of 15% butanol (P_{ButOH} = 0.14 kPa and P_{water} = 0.79 kPa) at 35 °C. The adsorption selectivity, determined by extracting the adsorbed concentrations of water and butanol from spectral data and using equation S2 (see the SI), was 606, showing that the film was highly butanol-selective. This selectivity value was significantly higher than that for the silicalite-1(OH^-) film, reported in our previous work to be 107,[30] showing that the silicalite-1(F^-) film has a much more hydrophobic nature. The adsorption of butanol from binary mixtures of butanol and water and the determination of the butanol/water selectivity will be the subject of further investigation.

CONCLUSIONS

A film composed of a monolayer of *b*-oriented silicalite-1 crystals was produced using seeds prepared with fluoride as a mineralizing agent and grown at nearly neutral pH using fluoride as a mineralizing agent for the first time. According to solid-state ^{29}Si MAS NMR and volumetric adsorption data, the number of structural defects in the form of polar silanol groups in these crystals was very small, thus demonstrating the hydrophobic nature of the crystals. Adsorption isotherms of water and butanol from the vapor phase were determined at four different temperatures. The butanol isotherms were typical of an adsorbate with a high affinity for a microporous material with a sharp increase in the amount adsorbed at low partial pressures. The Sips model was fitted to the butanol isotherms, and the model fit the experimental data well. The adsorption enthalpy determined was in concert with previous reports. Water, however, was adsorbed only in smaller amounts in the film at all temperatures studied, and the amounts adsorbed were comparable to the smallest amount ever reported for MFI-type zeolites, which confirms the true hydrophobic nature of silicalite-1 grown using fluoride as a mineralizing agent. According to the results obtained, silicalite-1(F^-) films seem to be very promising materials for the recovery of butanol from dilute aqueous mixtures.

ASSOCIATED CONTENT

Supporting Information

The Supporting Information is available free of charge on the ACS Publications website at DOI: 10.1021/acs.langmuir.6b03326.

In situ ATR-FTIR experiments and method, adsorption selectivity, and Sips and Langmuir isotherms (PDF)

AUTHOR INFORMATION

Corresponding Author

*E-mail: mattias.grahn@ltu.se.

Notes

The authors declare no competing financial interest.

ACKNOWLEDGMENTS

The authors acknowledge the Swedish Research Council (VR, under grant 621-2011-4060) for financially supporting this work. We acknowledge the Foundation in memory of J. C. and Seth M. Kempe for funding a Bruker IFS 66v/S FTIR spectrometer at LTU. All solid-state ^{29}Si MAS NMR experiments were performed by O.N.A. at the Magnetic Resonance Laboratory, Department of Physics, Warwick University, U.K. We thank Dr. James McDonald for advice in using a sample of a high-purity-grade kaolinite as an external reference in solid-state ^{29}Si NMR experiments and Dr. Daniela Rusanova for very useful discussions related to NMR results.

REFERENCES

(1) Caro, J.; Noack, M.; Kolsch, P. Zeolite membranes: From the laboratory scale to technical applications. *Adsorption* **2005**, *11* (3−4), 215−227.

(2) Remy, T.; Peter, S. A.; Van Tendeloo, L.; Van der Perre, S.; Lorgouilloux, Y.; Kirschhock, C. E.; Baron, G. V.; Denayer, J. F. Adsorption and separation of CO2 on KFI zeolites: Effect of cation type and Si/Al ratio on equilibrium and kinetic properties. *Langmuir* **2013**, *29* (16), 4998−5012.

(3) Long, Y. C.; Jiang, H. W.; Zeng, H. Sorbate/framework and sorbate/sorbate interaction of organics on siliceous MFI type zeolite. *Langmuir* **1997**, *13* (15), 4094−4101.

(4) Gascon, J.; Kapteijn, F.; Zornoza, B.; Sebastian, V.; Casado, C.; Coronas, J. Practical approach to zeolitic membranes and coatings: state of the art, opportunities, barriers, and future perspectives. *Chem. Mater.* **2012**, *24* (15), 2829−2844.

(5) Arruebo, M.; Falconer, J. L.; Noble, R. D. Separation of binary C-5 and C-6 hydrocarbon mixtures through MF1 zeolite membranes. *J. Membr. Sci.* **2006**, *269* (1−2), 171−176.

(6) Yu, L.; Korelskiy, D.; Grahn, M.; Hedlund, J. Very high flux MFI membranes for alcohol recovery via pervaporation at high temperature and pressure. *Sep. Purif. Technol.* **2015**, *153*, 138−145.

(7) Long, Y.-c.; Jiang, H.-w.; Zeng, H. Sorbate/framework and sorbate/sorbate interaction of organics on siliceous MFI type zeolite. *Langmuir* **1997**, *13* (15), 4094−4101.

(8) Milestone, N. B.; Bibby, D. M. Concentration of alcohols by adsorption on silicalite. *J. Chem. Technol. Biotechnol.* **1981**, *31* (1), 732−736.

(9) Bowen, T. C.; Noble, R. D.; Falconer, J. L. Fundamentals and applications of pervaporation through zeolite membranes. *J. Membr. Sci.* **2004**, *245* (1−2), 1−33.

(10) Stoeger, J. A.; Choi, J.; Tsapatsis, M. Rapid thermal processing and separation performance of columnar MFI membranes on porous stainless steel tubes. *Energy Environ. Sci.* **2011**, *4* (9), 3479−3486.

(11) Oudshoorn, A.; van der Wielen, L. A. M.; Straathof, A. J. J. Assessment of Options for Selective 1-Butanol Recovery from Aqueous Solution. *Ind. Eng. Chem. Res.* **2009**, *48* (15), 7325−7336.

(12) Maddox, I. Use of silicalite for the adsorption of n-butanol from fermentation liquors. *Biotechnol. Lett.* **1982**, *4* (11), 759−760.

(13) Richter, H.; Voß, H.; Voigt, I.; Diefenbacher, A.; Schuch, G.; Steinbach, F.; Caro, J. High-flux ZSM-5 membranes with an additional non-zeolite pore system by alcohol addition to the synthesis batch and their evaluation in the 1-butene/i-butene separation. *Sep. Purif. Technol.* **2010**, *72* (3), 388−394.

(14) Abdehagh, N.; Tezel, F. H.; Thibault, J. Multicomponent adsorption modeling: isotherms for ABE model solutions using activated carbon F-400. *Adsorption* **2016**, *22* (3), 357−370.

(15) Zhang, K.; Lively, R. P.; Zhang, C.; Chance, R. R.; Koros, W. J.; Sholl, D. S.; Nair, S. Exploring the framework hydrophobicity and flexibility of ZIF-8: from biofuel recovery to hydrocarbon separations. *J. Phys. Chem. Lett.* **2013**, *4* (21), 3618−3622.

(16) Cousin Saint Remi, J.; Rémy, T.; Van Hunskerken, V.; van de Perre, S.; Duerinck, T.; Maes, M.; De Vos, D.; Gobechiya, E.; Kirschhock, C. E.; Baron, G. V. Biobutanol Separation with the

DOI: 10.1021/acs.langmuir.6b03326
Langmuir 2016, 32, 11789−11798

Metal−Organic Framework ZIF-8. *ChemSusChem* **2011**, *4* (8), 1074−1077.
(17) Faisal, A.; Zarebska, A.; Saremi, P.; Korelskiy, D.; Ohlin, L.; Rova, U.; Hedlund, J.; Grahn, M. MFI zeolite as adsorbent for selective recovery of hydrocarbons from ABE fermentation broths. *Adsorption* **2014**, *20* (2−3), 465−470.
(18) Zhang, H.; Liu, D.; Yao, Y.; Zhang, B.; Lin, Y. Stability of ZIF-8 membranes and crystalline powders in water at room temperature. *J. Membr. Sci.* **2015**, *485*, 103−111.
(19) Park, K. S.; Ni, Z.; Côté, A. P.; Choi, J. Y.; Huang, R.; Uribe-Romo, F. J.; Chae, H. K.; O'Keeffe, M.; Yaghi, O. M. Exceptional chemical and thermal stability of zeolitic imidazolate frameworks. *Proc. Natl. Acad. Sci. U. S. A.* **2006**, *103* (27), 10186−10191.
(20) Meagher, M. M.; Qureshi, N.; Hutkins, R. Silicalite membrane and method for the selective recovery and concentration of acetone and butanol from model ABE solutions and fermentation broth. U.S Patent 5,755,967, 1998.
(21) Saravanan, V.; Waijers, D. A.; Ziari, M.; Noordermeer, M. A. Recovery of 1-butanol from aqueous solutions using zeolite ZSM-5 with a high Si/Al ratio; suitability of a column process for industrial applications. *Biochem. Eng. J.* **2010**, *49* (1), 33−39.
(22) Qureshi, N.; Hughes, S.; Maddox, I. S.; Cotta, M. A. Energy-efficient recovery of butanol from model solutions and fermentation broth by adsorption. *Bioprocess Biosyst. Eng.* **2005**, *27* (4), 215−222.
(23) Oudshoorn, A.; van der Wielen, L. A. M.; Straathof, A. J. J. Adsorption equilibria of bio-based butanol solutions using zeolite. *Biochem. Eng. J.* **2009**, *48* (1), 99−103.
(24) Huang, J. C.; Meagher, M. M. Pervaporative recovery of n-butanol from aqueous solutions and ABE fermentation broth using thin-film silicalite-filled silicone composite membranes. *J. Membr. Sci.* **2001**, *192* (1−2), 231−242.
(25) Bowen, T. C.; Li, S. G.; Noble, R. D.; Falconer, J. L. Driving force for pervaporation through zeolite membranes. *J. Membr. Sci.* **2003**, *225*, 165−176.
(26) Li, S.; Tuan, V. A.; Falconer, J. L.; Noble, R. D. Properties and separation performance of Ge-ZSM-5 membranes. *Microporous Mesoporous Mater.* **2003**, *58* (2), 137−154.
(27) Korelskiy, D.; Leppajarvi, T.; Zhou, H.; Grahn, M.; Tanskanen, J.; Hedlund, J. High flux MFI membranes for pervaporation. *J. Membr. Sci.* **2013**, *427*, 381−389.
(28) Zhou, H.; Korelskiy, D.; Leppajarvi, T.; Grahn, M.; Tanskanen, J.; Hedlund, J. Ultrathin zeolite X membranes for pervaporation dehydration of ethanol. *J. Membr. Sci.* **2012**, *399-400*, 106−111.
(29) DeJaco, R. F.; Bai, P.; Tsapatsis, M.; Siepmann, J. I. Adsorptive Separation of 1-Butanol from Aqueous Solutions Using MFI- and FER-Type Zeolite Frameworks: A Monte Carlo Study. *Langmuir* **2016**, *32* (8), 2093−2101.
(30) Farzaneh, A.; Zhou, M.; Potapova, E.; Bacsik, Z.; Ohlin, L.; Holmgren, A.; Hedlund, J.; Grahn, M. Adsorption of Water and Butanol in Silicalite-1 Film Studied with in Situ Attenuated Total Reflectance-Fourier Transform Infrared Spectroscopy. *Langmuir* **2015**, *31* (17), 4887−4894.
(31) Hunger, M.; Kärger, J.; Pfeifer, H.; Caro, J.; Zibrowius, B.; Bülow, M.; Mostowicz, R. Investigation of internal silanol groups as structural defects in ZSM-5-type zeolites. *J. Chem. Soc., Faraday Trans. 1* **1987**, *83* (11), 3459−3468.
(32) Koller, H.; Lobo, R. F.; Burkett, S. L.; Davis, M. E. SiO-. cntdot.. cntdot.. cntdot. HOSi Hydrogen Bonds in As-Synthesized High-Silica Zeolites. *J. Phys. Chem.* **1995**, *99* (33), 12588−12596.
(33) Zhang, K.; Lively, R. P.; Noel, J. D.; Dose, M. E.; McCool, B. A.; Chance, R. R.; Koros, W. J. Adsorption of water and ethanol in MFI-type zeolites. *Langmuir* **2012**, *28* (23), 8664−8673.
(34) Zhou, H.; Mouzon, J.; Farzaneh, A.; Antzutkin, O. N.; Grahn, M.; Hedlund, J. Colloidal defect-free silicalite-1 single crystals: preparation, structure characterization, adsorption and separation properties for alcohol/water mixtures. *Langmuir* **2015**, *31*, 8488−8496.
(35) Flanigen, E. M.; Patton, R. L. Silica polymorph and process for preparing same. U.S. Patent 4,073,865 A, 1978.
(36) Zhou, M.; Korelskiy, D.; Ye, P. C.; Grahn, M.; Hedlund, J. AUniformly Oriented MFI Membrane for Improved CO2 Separation. *Angew. Chem., Int. Ed.* **2014**, *53* (13), 3492−3495.
(37) Eroshenko, V.; Regis, R.-C.; Soulard, M.; Patarin, J. Energetics: A new field of applications for hydrophobic zeolites. *J. Am. Chem. Soc.* **2001**, *123* (33), 8129−8130.
(38) Mallon, E. E.; Jeon, M. Y.; Navarro, M.; Bhan, A.; Tsapatsis, M. Probing the relationship between silicalite-1 defects and polyol adsorption properties. *Langmuir* **2013**, *29* (22), 6546−6555.
(39) Qin, Z. X.; Lakiss, L.; Tosheva, L.; Gilson, J. P.; Vicente, A.; Fernandez, C.; Valtchev, V. Comparative Study of Nano-ZSM-5 Catalysts Synthesized in OH- and F- Media. *Adv. Funct. Mater.* **2014**, *24* (2), 257−264.
(40) Zhou, H.; Korelskiy, D.; Sjoberg, E.; Hedlund, J. Ultrathin hydrophobic MFI membranes. *Microporous Mesoporous Mater.* **2014**, *192*, 76−81.
(41) Zecchina, A.; Bordiga, S.; Spoto, G.; Marchese, L.; Petrini, G.; Leofanti, G.; Padovan, M. Silicalite Characterization 0.2. Ir Spectroscopy of the Interaction of Co with Internal and External Hydroxyl-Groups. *J. Phys. Chem.* **1992**, *96* (12), 4991−4997.
(42) Ohlin, L.; Bazin, P.; Thibault-Starzyk, F.; Hedlund, J.; Grahn, M. Adsorption of CO2, CH4, and H2O in zeolite ZSM-5 studied using in situ ATR-FTIR spectroscopy. *J. Phys. Chem. C* **2013**, *117* (33), 16972−16982.
(43) Grahn, M.; Holmgren, A.; Hedlund, J. Adsorption of n-hexane and p-xylene in thin silicalite-1 films studied by FTIR/ATR spectroscopy. *J. Phys. Chem. C* **2008**, *112* (20), 7717−7724.
(44) Wang, Z.; Larsson, M. L.; Grahn, M.; Holmgren, A.; Hedlund, J. Zeolite coated ATR crystals for new applications in FTIR-ATR spectroscopy. *Chem. Commun.* **2004**, *24*, 2888−2889.
(45) Grahn, M.; Wang, Z.; Lidström-Larsson, M.; Holmgren, A.; Hedlund, J.; Sterte, J. Silicalite-1 coated ATR elements as sensitive chemical sensor probes. *Microporous Mesoporous Mater.* **2005**, *81* (1), 357−363.
(46) Mohammed-Ziegler, I.; Hórvölgyi, Z.; Toth, A.; Forsling, W.; Holmgren, A. Wettability and spectroscopic characterization of silylated wood samples. *Polym. Adv. Technol.* **2006**, *17* (11−12), 932−939.
(47) Theunissen, E.; Kirschhock, C. E. A.; Kremer, S. P. B.; Habermacher, D. D.; Martens, J. A. Preferential Siting of Iron Atoms in an MFI-type Ferrisilicate Zeolite Framework: An Attempt to Explain Experimental Data with TPA-Silicate Solution Chemistry. *Eur. J. Inorg. Chem.* **2003**, *2003* (7), 1296−1298.
(48) Villaescusa, L.; Díaz, I.; Barrett, P.; Nair, S.; Lloris-Cormano, J.; Martínez-Mañez, R.; Tsapatsis, M.; Liu, Z.; Terasaki, O.; Camblor, M. Pure silica large pore zeolite ITQ-7: synthetic strategies, structure-directing effects, and control and nature of structural disorder. *Chem. Mater.* **2007**, *19* (7), 1601−1612.
(49) Koller, H.; Wölker, A.; Villaescusa, L.; Diaz-Cabanas, M.; Valencia, S.; Camblor, M. Five-coordinate silicon in high-silica zeolites. *J. Am. Chem. Soc.* **1999**, *121* (14), 3368−3376.
(50) Brito e Abreu, S.; Skinner, W. Determination of contact angles, silane coverage, and hydrophobicity heterogeneity of methylated quartz surfaces using ToF-SIMS. *Langmuir* **2012**, *28* (19), 7360−7367.
(51) Wenzel, R. N. Surface Roughness and Contact Angle. *J. Phys. Colloid Chem.* **1949**, *53* (9), 1466−1467.
(52) Yee, G. G.; Fulton, J. L.; Smith, R. D. Fourier-Transform Infrared-Spectroscopy of Molecular-Interactions of Heptafluoro-1-Butanol or 1-Butanol in Supercritical Carbon-Dioxide and Supercritical Ethane. *J. Phys. Chem.* **1992**, *96* (15), 6172−6181.
(53) Sips, R. On the structure of a catalyst surface. *J. Chem. Phys.* **1948**, *16* (5), 490−495.
(54) Do, D.; Do, H. D. A new adsorption isotherm for heterogeneous adsorbent based on the isosteric heat as a function of loading. *Chem. Eng. Sci.* **1997**, *52* (2), 297−310.
(55) Lee, J.-H.; Thio, B. J. R.; Bae, T.-H.; Meredith, J. C. Role of Lewis basicity and van der Waals forces in adhesion of silica MFI zeolites (010) with polyimides. *Langmuir* **2009**, *25* (16), 9101−9107.

DOI: 10.1021/acs.langmuir.6b03326
Langmuir 2016, 32, 11789−11798

(56) Qureshi, N.; Blaschek, H. P. Recovery of butanol from fermentation broth by gas stripping. *Renewable Energy* **2001**, *22* (4), 557−564.
(57) Zhang, K.; Lively, R. P.; Dose, M. E.; Brown, A. J.; Zhang, C.; Chung, J.; Nair, S.; Koros, W. J.; Chance, R. R. Alcohol and water adsorption in zeolitic imidazolate frameworks. *Chem. Commun.* **2013**, *49* (31), 3245−3247.
(58) Einicke, W.-D.; Messow, U.; Schöllner, R. Liquid-phase adsorption of n-alcohol/water mixtuers on zeolite NaZSM-5. *J. Colloid Interface Sci.* **1988**, *122* (1), 280−282.
(59) Jentys, A.; Warecka, G.; Derewinski, M.; Lercher, J. A. Adsorption of water on ZSM 5 zeolites. *J. Phys. Chem.* **1989**, *93* (12), 4837−4843.
(60) Jentys, A.; Tanaka, H.; Lercher, J. Surface processes during sorption of aromatic molecules on medium pore Zeolites. *J. Phys. Chem. B* **2005**, *109* (6), 2254−2261.

DOI: 10.1021/acs.langmuir.6b03326
Langmuir 2016, 32, 11789−11798